Molecular Dynamics Simulation of an Amorphous Polymer under Tension. 1. Phenomenology

David Brown* and Julian H. R. Clarke

Chemistry Department, U.M.I.S.T., Manchester M60 1QD, U.K.

Received August 28, 1990; Revised Manuscript Received October 25, 1990

ABSTRACT: Molecular dynamics computer simulation has been used to study the properties of a linear polymer model resembling polyethylene over a wide range of temperatures. A loose coupling constant pressure method was used to facilitate examination of mechanical properties between 10 and 500 K. By applying uniaxial tension to the samples, we have characterized elasticity, yield, and plastic flow at low temperatures and viscoelasticity at high temperatures. Qualitative comparisons show that there are strong similarities between these short time (~1 ns) simulations and laboratory measurements obtained on time scales orders of magnitude longer. The extensional (Young's) modulus has values typical of a glassy solid for $T \leq 100$ K and shows a significant decrease as the temperature is raised. The high temperature of the glass transformation, as characterized by the disappearance of a yield stress, and the breadth of the transformation region, as characterized by density and modulus, are both explained in terms of the ultrashort time scale of the computer experiments.

1. Introduction

In this paper we present and discuss the results of molecular dynamics (MD) computer simulations in which we explore mechanical properties of a model dense amorphous polymer by determining directly the response to the application of a uniaxial tension. Although the model resembles polyethylene, the aim of the work was not primarily to reproduce the properties of any real material. Rather we wished to explore the behavior of a simple polymer model that incorporates the essential properties of connectivity, restricted flexibility, and van der Waals interactions and to establish to what extent mechanical properties determined for small samples on the very short time scale of simulations relate to properties of real polymers as studied in the laboratory. In a forthcoming paper we will interpret the results in terms of the microscopic properties of the material.

We have probed both the linear and nonlinear behavior of this model and show that the phenomena observed display similarities to results obtained in the laboratory on time scales many orders of magnitude longer. The simulations were performed at several temperatures and demonstrate the gradual transition from glassy to fluid behavior.

There is a general recognition of the need for an atomistic description of polymer chains when modeling glassy materials where the effects of restricted intramolecular motions and chain interactions are in strong competition with entropic effects. The mechanical properties of polymers are fundamental in the majority of their practical applications and the long-term objective is to use monomer level modeling to promote further understanding and eventually to provide accurate prediction of properties without resort to expensive synthesis and testing procedures. Scaling concepts such as have been so valuable for polymers in other regimes (e.g., melts or dilute solutions) have yet to be developed for dense amorphous polymers. For instance, although it is known that glass transition phenomena are related to chain flexibility, quantitative theoretical predictions are currently not possible.

Several approaches to the modeling of dense polymers have been proposed in recent years. Energy minimization techniques have been used extensively to explore the mechanical properties of polypropylene.[1,2] These simulations are effectively at 0 K and rest on the assumption that entropic effects can be completely ignored in modeling the mechanical response of the samples. Other authors have used finite temperature molecular dynamics to investigate amorphous systems of alkane chains[3,4] and also simple model networks.[5]

In an earlier article[6] we described molecular dynamics simulations of amorphous and ordered microstructures of a model oriented polymer fiber using a lamina model in which the linear chains were suspended between two parallel plates representing the faces of adjacent crystallites. More recently[7] we introduced a novel molecular dynamics method for simulating dense polymers. It is an adaptation of the loose coupling algorithm proposed by Berendsen et al.,[8] which allows the shape and size of the primary MD cell to adjust to imbalances between an externally applied tensorial pressure field and that measured internally. The method not only enables us to bring samples to "equilibrium" under conditions of an isotropic pressure but also facilitates nonequilibrium experiments of the kind to be described here. Although the theoretical basis of the loose coupling approach has been criticised,[9,10] it has been found for fluid systems[10] that to within statistical uncertainties the first-order properties are identical with those obtained by more rigorous approaches.[9,11,12] An extended ensemble method has been recently used to perform constant temperature and pressure tensor MD simulations of an amorphous dense polymer.[13] In section 2 we shall argue, however, that the loose coupling approach offers a more practical approach to studying the properties of polymer samples.

In this paper we describe results obtained for a single linear polymer chain of $N = 1000$ sites that forms a dense amorphous polymeric system through the replicative properties of periodic boundaries. The continuous (primary) chain is not confined to the primary MD cell but can span neighboring cells. The model is therefore one of a monodisperse polymer entangled with replicas of itself. For small N there is no doubt that the model gives a poor representation of bulk behavior but as N becomes larger we expect it to be an increasingly better approximation to a dense amorphous system. With $N = 1000$ the size of the chain should be several times the entanglement length of this polymer.

Polymer samples were generated by using a modified self-avoiding random walk performed within the confines

0024-9297/91/2224-2075$02.50/0

of the periodic boundary conditions, followed by dynamical relaxation at constant pressure. We discuss elsewhere various alternative prescriptions for building an amorphous structure close to mechanical equilibrium at a required temperature.[14] Each sample so prepared is just one of many possible configurational microstates of the polymer that can exist under the prescribed conditions. To obtain results that are representative of the bulk polymer it is therefore necessary to average results obtained for several independent configurations.

In the following section we give a brief outline of a loose coupling constant pressure MD technique, originally proposed by Berendsen et al.,[8] that we have adapted and extended for use on polymer samples. The implementation of this technique has been described in detail elsewhere.[7] In section 3 information concerning the choice of potential parameters is given and in sections 4 and 5 the results are presented and discussed.

2. Loose Coupling Constant Pressure Molecular Dynamics

The method used[7,8] involves weak coupling of an external tensorial pressure field, $\mathbf{P}^0$, to the system through a simple feedback loop. The coupling is implemented by allowing the matrix $\mathbf{h}$, made up from the basis vectors $\mathbf{a}$, $\mathbf{b}$, and $\mathbf{c}$, which determine the shape and size of the primary dynamics cell, to respond to imbalances between the internally measured pressure tensor, $\mathbf{P}$, and the externally applied pressure tensor, $\mathbf{P}^0$. (We prefer the use of the pressure tensor notation to that of the alternative stress tensor, σ. The generally accepted convention and that use here is that $\sigma = -\mathbf{P}$ but unfortunately there is some ambiguity in the term "stress" since in some texts, e.g., ref 15, σ is defined as being equal to $+\mathbf{P}$.)

We have modified the original method to ensure that $\mathbf{h}$ remains symmetric throughout by defining the equation for the rate of change of the $\mathbf{h}$ matrix with time to be

$$\dot{\mathbf{h}} = \frac{\mathbf{P} - \mathbf{P}^0}{M} \tag{1}$$

$\mathbf{P}$ is the internally measured pressure tensor, which in this case is defined to be symmetric

$$\mathbf{P} = \frac{1}{V}\sum_{i=1}^{N}\left[\frac{1}{m_i}\mathbf{p}_i\mathbf{p}_i + \mathbf{r}_i\mathbf{f}_i\right] \tag{2}$$

where V is the volume and m_i, $\mathbf{p}_i$, $\mathbf{r}_i$, and $\mathbf{f}_i$ are the mass, momentum, position, and force on the ith site, respectively. M is an empirically chosen coupling constant with a value of 5.25×10^6 Pa s m^{-1}, we describe elsewhere[7] the criteria used for choosing the value of M so that the coupling has an insignificant effect on the first-order properties of the system.

As in the loose coupling method[8] and other "constant pressure" schemes[9,11] a simple proportional scaling of coordinates is used to minimize local disturbances. So defining a set of scaled coordinates, $\mathbf{s}$, by

$$\mathbf{s} = \mathbf{h}^{-1}\mathbf{r} \tag{3}$$

and differentiating give the following equation of motion for the sites

$$\dot{\mathbf{r}}_i = \mathbf{h}\dot{\mathbf{s}}_i + \dot{\mathbf{h}}\mathbf{s}_i = \frac{\mathbf{p}_i}{m_i} + \dot{\mathbf{h}}\mathbf{h}^{-1}\mathbf{r}_i \tag{4}$$

The motion is thus seen to be split into two contributions that are integrated separately, that due to the momenta and that resulting from the change in shape and size of the cell. The "fast" motions due to the momenta are dealt with in the usual way by using a "leapfrog" algorithm incorporating an iterative scheme to maintain the bond length constraints, whereas a simple first-order Taylor expansion is considered sufficient to integrate the equation for the relatively "slow" motion of the box

$$\mathbf{h}(t + \Delta t) = \mathbf{h}(t) + \left[\frac{\mathbf{P} - \mathbf{P}^0}{M}\right]\Delta t \tag{5}$$

It can then simply be shown that to first order the motion of the box results in a scaling of the position of a site

$$\mathbf{r}_i(t + \Delta t) = \mathbf{h}(t + \Delta t)\mathbf{h}^{-1}(t)\mathbf{r}_i(t) = \mathbf{H}\mathbf{r}_i(t) \tag{6}$$

As compared to the more rigorous Rahman–Parrinello (RP) technique,[11] loose coupling does have important practical advantages. The pressure imbalance is coupled to the *first derivative* of the basis vectors rather than to the second derivative (as in the RP technique), which means that motions of the box are overdamped and so there is little tendency for an unphysical oscillatory response to changes in the applied pressure. For this reason the above method is to be preferred when the nonequilibrium properties of dense highly viscoelastic systems are of interest. Also the method is extremely simple to implement, since it is compatible with the simple second-order integration algorithms much in use in MD.

As we have pointed out in the Introduction an extended ensemble RP-type method has been implemented for a dense polymer system where the atomic pressure tensor has had to be used and where the model of the polymer employs rigid bond constraints.[13] The technique can be modified[16] by including an extra damping term to prevent an oscillatory response from occurring when a pressure perturbation is applied but of course this removes the rigor of the method.

3. Details of the Model and Simulations

In our polyethylene-like polymer each of the 1000 monomer units is treated as a single site and is given a mass corresponding to that of a CH_2 group. Neighboring sites on the chain are connected together by rigid bonds of length $b_0 = 0.153$ nm. Flexibility of the chains is limited by incorporating a harmonic valence angle potential, $\Phi(\theta)$, and a torsional potential, $\Phi(\alpha)$, into the model. $\Phi(\theta)$ is of the form

$$\Phi(\theta) = (1/2)k_\theta(\cos\theta - \cos\theta_0)^2 \tag{7}$$

where $k_\theta = 520$ kJ mol^{-1} and $\theta_0 = 112.813°$. We use the cosine of the angle in the harmonic potential for computational convenience. Other workers have expressed $\Phi(\theta)$ directly in terms of angle displacements[17] using the same value of k_θ. For small displacements there is very little difference in the two models. In any case in the absence of precise experimental data the choice of k_θ is somewhat arbitrary.

The torsional potential restricting internal rotations about a bond in the chain is parametrized in terms of the dihedral angle, α, formed by this bond and the two adjacent bonds. The exact form used is that due to Steele[18] and is given as

$$\Phi(\alpha)/\text{J mol}^{-1} = C_0 + C_1\cos\alpha + C_2\cos^2\alpha + C_3\cos^3\alpha \tag{8}$$

where $C_0 = 8832$, $C_1 = 18\,087$, $C_2 = 4880$, and $C_3 = -31\,800$. Finally, nonbonded monomer interactions, i.e., those between sites separated by at least three others, are represented by a Lennard-Jones (LJ) 12-6 potential with $\epsilon/k_B = 57$ K and $\sigma = 0.428$ nm. These parameters are the

same as those given before[7] and give a reasonable fit to the density of real polyethylene at 500 K as obtained by extrapolating the data of Richardson et al.[19]

During the dynamical simulations the temperature was controlled by the constant temperature loose coupling method previously discussed[7,8] with a coupling constant τ_T of 1 ps. As for M the choice for the value of τ_T has been discussed in detail already.[7] The LJ 12-6 potential was truncated at $r_c = 2.5\sigma$ and the appropriate long-range corrections were made to the potential energy and the virial at each step according to the density and assuming $g(r) = 1$ for $r > r_c$. A check was also made at each step to ensure that the perpendicular distance between any of the opposite faces of the primary cell did not drop below $2r_c$. This is important as the cell can distort significantly away from its cubic origins, especially when subjected to anisotropic pressure fields. To calculate the LJ interactions more efficiently a standard Verlet neighbor list technique[20] was used. Further details of how this was implemented and optimized have already been given.[7]

In the algorithm used to integrate the equations of motion[7] the time step used was 2.5 fs when the temperature required was ~400 K or higher but was increased to 5 fs for simulations carried out at 300 K and below. The bond constraints were maintained to a relative tolerance of 10^{-6} by using an iterative scheme. The reconciliation of using a constrained bond length in a simulation where coordinates are constantly being rescaled to facilitate changes in the shape and size of the primary cell has been addressed previously[8] and is discussed in great detail in ref 7.

The basic algorithm was tested under (N,V,E) conditions with the $N = 1000$ site model as described except that the LJ potential was truncated at the minima and raised by an amount ϵ so as to avoid problems with the discontinuities in force and potential in using the usual truncation radius. A 100 000-step (N,V,E) simulation carried out at ~400 K using a time step of 2.5 fs revealed that the root mean square fluctuations in the total energy were less than 1% of those in the total potential energy and the drift in total energy was about 1 part in 10 000 during the 250-ps run.

All the simulations were performed either on the Amdahl VP1200 at the Manchester Computing Centre, using programs optimized to take advantage of its vector architecture, or on a Silicon Graphics 260 GTX Power Series machine. Each time step consumed approximately 0.054 s of cpu time on the VP. The corresponding cpu time for code scalar optimized to run on one processor of the SG 260 GTX is ~2.2 s.

4. Sample Preparation and Dynamic Relaxation

A common method of preparing equilibrium samples of atomic liquids for computer simulations is to melt a crystal configuration. As the system melts the short correlation lengths involved and the mobility of the atoms ensure that an isotropic liquid structure is formed within a relatively short space of time. Long correlation lengths and low mobility ensure that this approach is a totally impractical way of generating a sample of amorphous polymer. Instead it is necessary to build in the computer an amorphous structure that is already close to equilibrium as near to the required density as possible. For this purpose we have used a modified self-avoiding random walk performed within the confines of the periodic boundary conditions.

As described in detail before[21] the method generates the linear chain sequentially site by site with an acceptance

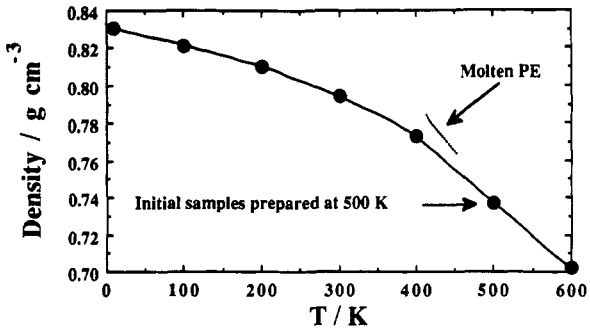

Figure 1. Average density of the polymer model at a pressure of 1 bar as a function of temperature. The initial samples were grown and relaxed at 500 K by using the method described in the text. Samples at other temperatures were prepared by heating or cooling at a rate of 1 K ps^{-1} (see text for details). The Lennard-Jones potential parameters were adjusted to give a density at 500 K that corresponds approximately to the extrapolation of experimental data for molten polyethylene (dotted line).[19] The spread in the results from the five independent samples is less than the size of the symbols.

criterion very similar to the Monte Carlo method. At each step a new proposed site is generated by first of all choosing an intended dihedral angle, α ($\alpha = 0$ implies trans), using a random number generator. The proposed position, $\mathbf{r}_{i+1}$, is then calculated from the three previous sites in accordance with the equilibrium bond length, b_0, the valence angle, θ_0, and the random dihedral angle. If the new position lies outside the primary cell, then its image within the cell is calculated in the usual way. The change in energy, $\Delta\Phi$, caused by introducing this site is then determined by summing up all new interactions, using the minimum image convention, and adding to this the new contribution to the dihedral angle energy, $\Phi(\alpha)$. The Boltzmann factor of this energy change, $\exp(-\Delta\Phi/k_BT)$, is then compared to another random number between 0 and 1. If the random number is less than the Boltzmann factor, then the new site is accepted, otherwise it is rejected and a new proposed site is generated. Should repeated trials (50) fail to find an acceptable position for the new site the chain is shortened by one site and the process starts afresh by attempting to generate a new $\mathbf{r}_i$ and if successful a new $\mathbf{r}_{i+1}$. If the chain again cannot find a suitable $\mathbf{r}_{i+1}$ then the chain is shortened this time by two sites and so on until an acceptable configuration is found. This process continues until all N sites have been generated.

A general problem with this kind of method is that as sites are added the effective volume available to subsequent ones diminishes. Thus sites generated toward the end "see" a very different environment than those at the start and a bias is detectable in the variation of the fraction of dihedral angles in the trans state as a function of the position along the chain. Once the chain is dynamically relaxed, however, the initial biases disappear so their use, at least for this linear chain model, is considered justified.

Five independent samples were generated and allowed to relax for 500 ps at 500 K at an applied isotropic pressure of 1 bar. Configurations at lower temperatures were obtained by cooling these samples at a rate of 1 K ps^{-1} to the desired temperature, again under conditions of constant applied isotropic pressure of 1 bar, followed by a subsequent period of relaxation of order 1 ns. By use of this procedure samples were generated at 500, 400, 300, 200, 100, and 10 K. In addition one sample only was heated in an analogous manner to 600 and 1000 K.

The mean densities obtained at the various temperatures are shown in Figure 1. As the temperature is lowered

from 500 K the density is seen to increase with a gradual decrease in the thermal expansivity of the polymer (obtained from the slope of the plot) toward values typical of amorphous solids. It is not easy to make useful comparisons with data on real polyethylene since the laboratory material is very difficult to prepare in a completely amorphous state. Data exist only for a narrow temperature range of the polyethylene melt[19] and as stated above use of the chosen chain interaction parameters results in a reasonable fit to the density at 500 K. Although we might expect the expansivity to increase at higher temperatures, our data for 500 and 600 K suggest that the model polymer has a much lower expansivity than the laboratory material; deficiencies in the model for polyethylene and incomplete relaxation even at the higher temperature could both contribute to this effect. On this basis it is not surprising that upon cooling below 500 K the density of the modeled material is much lower than that of real polyethylene.

The decrease in expansivity as the sample is cooled is exactly as expected upon glass formation; the relaxation in density cannot keep up with the rate of removal of kinetic energy as the sample is cooled and it falls progressively further out of equilibrium. The apparent broad nature of the transformation range is understandable in view of the very rapid effective cooling rate amounting to about 10^{11} K s^{-1} in the simulation experiment. We return to this point again later in the discussion.

5. Tension Experiments

(a) Nonlinear Behavior. To investigate the mechanical properties the sets of relaxed samples at each of the five temperatures were subjected to a gradually increasing uniaxial tension by changing the y component of the *applied* pressure tensor, P^0_{yy}, at a constant rate

$$dP^0_{yy}/dt = -\dot{\tau} \tag{9}$$

where the tension application rate, $\dot{\tau}$, used was either 5 or 1 bar ps^{-1} and the minus sign accounts for the fact that tension is a negative pressure. Employing two different values for $\dot{\tau}$ is useful in gauging the extent to which the measured properties are rate dependent.

In the results to be described we shall be interested primarily in the strain induced in the sample. The applied tension is then best considered as a control variable that produces a change in the strain, the response to which is the *measured* tension. In our experiments both the strain and the tension are dependent variables. The method is preferable to direct control of the strain since there is no way a priori of predicting how the shape or density of the sample will respond to a change in the external conditions. Studies have recently been reported of polymer deformation using energy minimization at constant volume,[2] a restriction that imposes a value of 0.5 for Poisson's ratio. This is equivalent to applying a complex pressure field that makes interpretation and comparison with real systems more difficult.

Experiments were generally continued until the sample had extended by about 50–100% of its original length. With such small samples extension beyond about 100% is not possible without violating the truncation radius criterion for the site–site potential due to the contraction in the transverse direction.

The primary information that results from these tension experiments is the response of the **h** matrix, defining the size and shape of the primary cell, and that of the internal pressure tensor, **P**. These together allow us to elucidate the stress versus strain behavior. In general the small system sizes used mean that there is a relatively complex and fluctuating response of the shape and dimensions of the system to the applied tension. Rather than present a bewildering mass of information on cell lengths and angles, we have used the **h** matrix to calculate the length of the primary cell, L, parallel to the direction of the applied tension and the cross-sectional area, A, perpendicular to it. From A an effective width, W, can also be defined

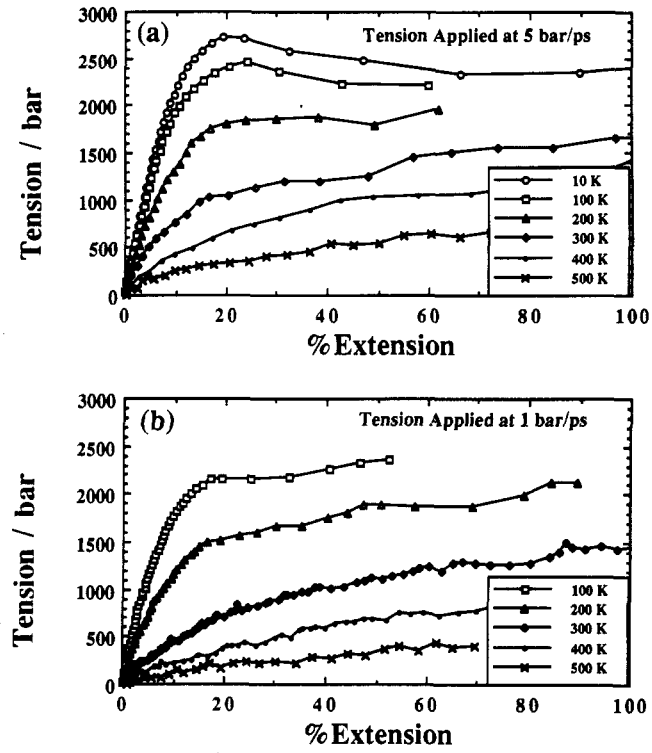

Figure 2. Measured tension ($-P_{yy}$) as a function of percentage extension ($\gamma_L \times 100$) for tension applied at (a) 5 and (b) 1 bar ps^{-1}. The data at each temperature represent the average behavior over five independent samples.

$$W = A^{1/2} \tag{10}$$

Using L and W the effect of the applied tension can be resolved into the nominal strains parallel and perpendicular to the direction of application in the same way as would happen in a laboratory experiment

$$\gamma_L = \frac{L - L_0}{L_0} \tag{11}$$

$$\gamma_W = \frac{W - W_0}{W_0} \tag{12}$$

Here the zero subscript denotes the equilibrium value and is defined in this case as the average over a time interval of about 100 ps just prior to the application of tension.

In Figure 2 the measured tension, i.e., $-P_{yy}$, is plotted against the percentage extension ($100\gamma_L$) for all the experiments carried out with the two tension application rates of 1 and 5 bar ps^{-1}; each set of data is the average of all five independent samples. To obtain the mean curves, the data from the different samples have been averaged with respect to time, i.e., the independent variable. Figure 2 clearly demonstrates the range of behavior observable in the model system. At low temperatures the material can support the tension up to strains of ~20% before undergoing yield. At progressively higher temperatures there is a gradual change in behavior until

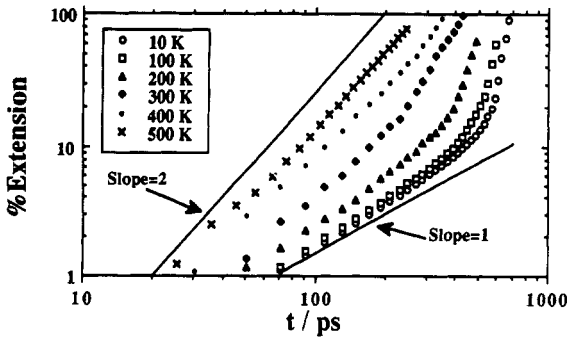

Figure 3. Percentage extension as a function of time for the samples subjected to a tension application rate of 5 bar ps^{-1}. On the log–log plot a slope of 1 indicates an elastic response to the applied tension, whereas a slope of 2 is that expected of a viscous material (see the text for details).

at 500 K it is unclear from Figure 2 whether there is any elastic response at all.

Plotting the extension against time demonstrates the difference between elastic and viscous behavior as shown in Figure 3. On the log–log scale an elastic response should have an asymptotic slope of 1 at low strains for a system with a well-defined Young's modulus, E

$$-P_{yy} = E\gamma_L \tag{13}$$

Alternatively if the response to the applied tension is viscous, i.e.

$$-P_{yy} = \eta_e\dot{\gamma}_L \tag{14}$$

where η_e is an elongational viscosity coefficient, then it is easy to show for the experiment we perform here that the strain would increase quadratically in time and hence give a slope of 2 in Figure 3. Both types of behavior are evident, confirming the trend from elastoplastic to viscous response as the temperature is increased. The estimated extensional viscosity at 500 K from the simulations is on the order of 0.01 Pa s. Although this is much lower than the equilibrium extensional viscosity of polyethylene, it is known that the viscosity does decrease significantly with increasing strain rate.[22] At the extension rates used in our simulations, $10^7 \rightarrow 10^9$ s^{-1}, we expect the behavior to be similarly non-Newtonian.

In the laboratory it is not easy to measure the true tension in a macroscopic sample due to the inhomogeneity in the distribution of stress and strain[23] that accompanies necking and cold-drawing. The more usual plot in this case is of the load versus extension in which yield is often accompanied by a noticeable load drop. If we take the product of the measured tension, $-P_{yy}$, and the effective cross-sectional area, A, then a pseudoload can be calculated. In Figure 4 this load has been plotted for all the data obtained at the two different tension application rates. For our systems the dimensions of the cell are only of order 30 Å so the loads obtained appear small, $\sim 10^{-9}$ N, in comparison to laboratory values. The load drop is quite evident in the plot for the tension applied at 5 bar ps^{-1} at a temperature of 200 K and below. Ward and Brown[24] suggest that there is a drop in true tension at the yield point; this is supported by our data at 5 bar ps^{-1} but not by that for the lower tension application rate.

The observed values of the yield stress and strain are much larger than those typically observed in the laboratory. In qualitative terms we can understand this as the result of the slow response of the internal structure as compared to the time scale of the perturbation. In comparing parts a and b of Figure 2 and parts a and b of Figure 4, it is evident that there is a decrease in the values of both the

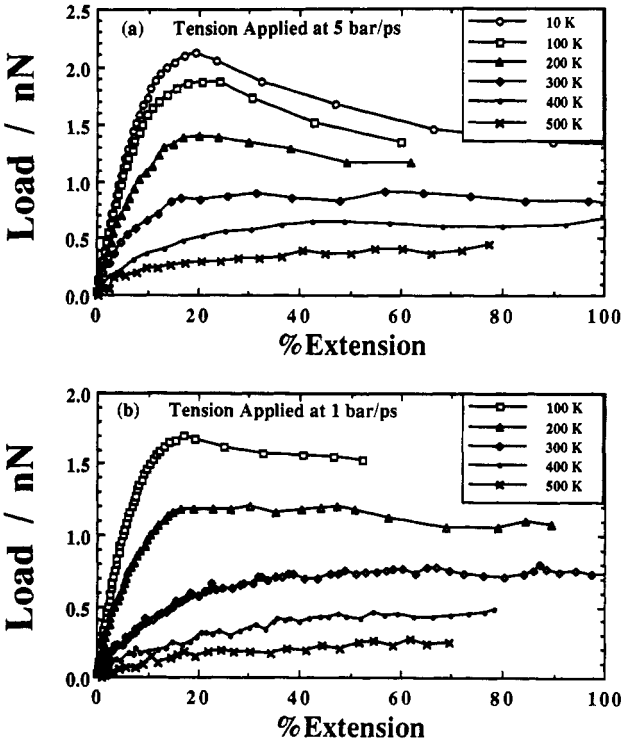

Figure 4. Load as a function of percentage extension ($\gamma_L \times 100$) for tension applied at (a) 5 and (b) 1 bar ps^{-1}.

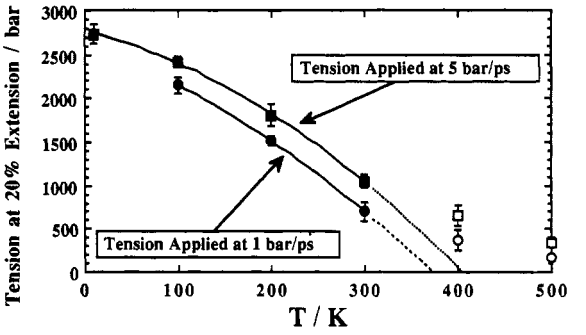

Figure 5. Tension at 20% extension (yield stress) as a function of temperature. Squares and circles refer to tension application rates of 5 and 1 bar ps^{-1}, respectively. Open symbols indicate data for which no discernible yield was observed; these points are excluded from the curve fits and extrapolations to zero tension. The error bars shown are the standard deviations in the results for the five independent samples.

yield stress and the yield strain as the tension application rate (or strain rate) is decreased, behavior that is analogous to that of real polymeric materials.[25]

One working definition of the yield stress in the laboratory is the true stress at the maximum observed load.[26] For convenience we have chosen to define the yield stress as the measured tension at a strain of 20%, which corresponds closely to observed maxima in the load for those samples that show a maximum. The resultant values are plotted in Figure 5 and the behavior is very similar to that found in real systems where the yield stress decreases approximately linearly with increasing temperature.[27] Our data covers a very wide temperature range, which may account for the slight nonlinearity. It has also been shown in laboratory experiments that extrapolating data to zero yield stress results in a convergence to a temperature close to the glass transition temperature.[27] If we ignore the points above 300 K for which there is no discernible yield point, our data extrapolate to zero yield stress at temperatures in the region of 400 K. As for laboratory measurements there is a dependence on the rate of

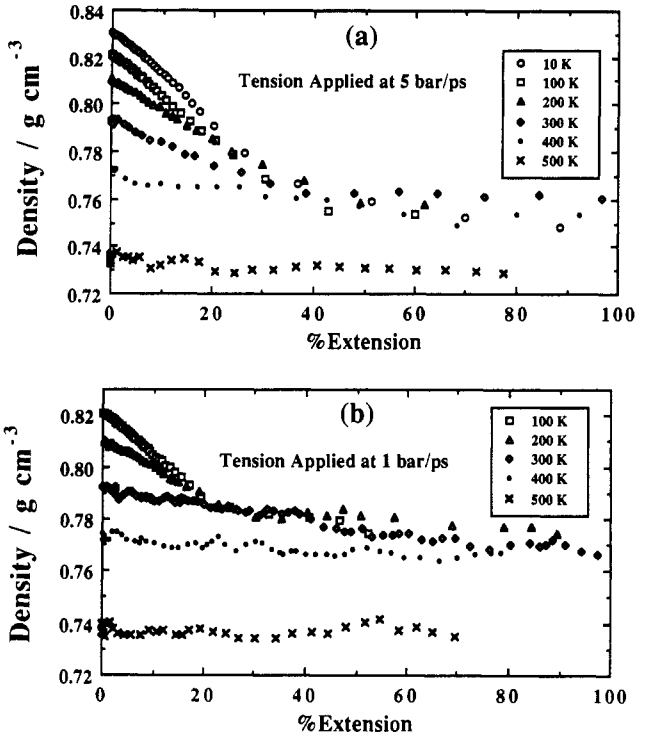

Figure 6. Behavior of the density during the extension experiments for tension application rates of (a) 5 and (b) 1 bar ps^{-1}. Note the distinct density decrease as the extension approaches the yield point at the lower temperatures. This contrasts with postyield plastic flow and the viscous flow observed at high temperatures.

application of the tension with the lower rate leading to consistently lower values of the yield stress and hence a lower extrapolated temperature of zero yield stress.

We can gain some insight into the nature of the yield process by examining the response of the system densities to the applied tension at the different temperatures. At high temperatures (400–500 K) where the flow process is predominantly viscous there is a hardly perceptible change in density during the extension of the samples (see Figure 6). In contrast at low temperatures there is a noticeable dilation effect as the tension is applied and the density decrease continues until just beyond the yield point. Once the material yields the density remains relatively constant as plastic flow takes place. What is interesting is that for a given tension application rate this apparent critical density for yield and plastic flow is *independent* of temperature over the range 10–300 K.

The convergence of the density curves to a "critical density" close to the yield strain supports the notion that for a particular extension rate the process at the actual point of yield is a constant density phenomenon. There is also a detectable dependence of this critical density upon the rate of application of the tension with the value varying from ~0.76 g cm^{-3} at 5 bar ps^{-1} and increasing to ~0.78 g cm^{-3} at 1 bar ps^{-1} with a corresponding change in the value of the extension at which this point is reached from about 30% to 20%. The decrease in density under extension at the lower temperatures is entirely consistent with the typical values of Poisson's ratio (μ) for amorphous polymeric solids, which are generally in the range 0.3–0.4.[28] Indeed our estimates of Poisson's ratio from the extensional and contractile strains

$$\mu = \lim_{\gamma_L \to 0} (-\gamma_C/\gamma_L) \tag{15}$$

give values of about 0.41 at the lowest temperatures.

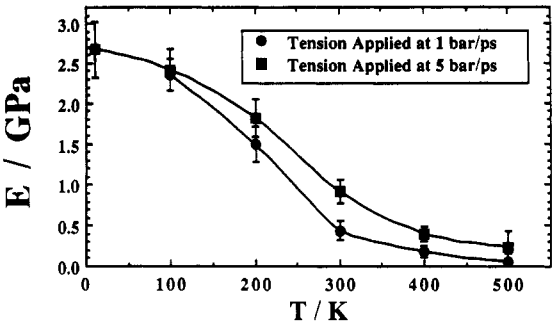

Figure 7. Extensional (Young's) modulus obtained from small (<5%) strain behavior (see text) as a function of temperature. The squares and circles refer to the data obtained at tension application rates of 5 and 1 bar ps^{-1}, respectively.

(b) Extensional Modulus. The extensional and shear moduli are important properties, which quantify the mechanical response of a polymer in the linear, small strain regime. In the laboratory generally a dynamic technique is used in which an oscillating small amplitude strain is applied to a sample at a certain frequency and the components of the (complex) moduli are then determined from the amplitude and phase lag of the resultant stress. As a function of decreasing temperature a significant change in the storage (real) modulus usually accompanies the transition to glassy-type behavior. Although our experiments are carried out in a different manner, it is still possible to obtain a modulus from the initial slopes of the tension versus extension plots.

Young's modulus is defined as the ratio of stress to strain in the limit of zero strain. It is, however, difficult to obtain precise values of this quantity from the experiments, in our case due to the increasingly poor statistics of the points at low extensions. As a compromise we have determined values of the modulus from a least-squares fit of the tension versus extension data for those points having an extension less than 5%. This procedure is somewhat arbitrary but only at the very lowest temperatures can an obvious nonlinear trend be seen in these plots (not shown). In this paper we are not primarily concerned with the exact values of the modulus but more with the trend as a function of temperature and tension application rate, so we do not consider this to be a significant problem. In Figure 7 the average moduli obtained at the different temperatures from the experiments at both applied tension rates are shown. To give an indication of the errors involved, the standard deviations evaluated from the five samples are also shown.

The convergence of the moduli at the lowest temperatures is expected as the material becomes more solidlike. At higher temperatures lower values of the modulus occur for the lower tension application rate, emphasizing the viscoelastic nature of the response. The results of our very rapid experiments should best be compared with high-frequency experimental data, but at low temperatures the moduli are relatively insensitive to frequency. The actual values of the modulus at low temperatures are of the same order as those measured in the laboratory (~10^9 Pa).[29] At higher temperatures (400 and 500 K) the moduli fall to relatively small values, although the decrease is much smaller than the 3 or 4 orders of magnitude decrease that is seen in the laboratory. It is, however, unlikely that we would be able to measure such a large decrease due to statistical problems.

(c) The Glass Transformation. The glass transition arises from failure of a system to achieve full thermodynamic equilibrium during continuous cooling. It is a

kinetic phenomenon determined by the temperature dependence of characteristic structural relaxation processes in the material.

The characterization in our simulations of a gradual change from fluid to solid behavior as the temperature is lowered suggests that the model material has undergone some kind of glass transformation. At first sight the characteristics are quantitatively quite different from what is observed on macroscopic time scales in the laboratory. As a result of experimental difficulties in realizing the pure amorphous polymer in the laboratory we can only estimate T_g, as values found in the literature are in the range ~150–300 K.[30] It is evident, however, from extrapolations to zero yield stress that the transition is taking place at a much higher temperature than one would expect and from the behavior of the modulus the transition region seems to extend over a very wide range of temperature (~200 K).

We can account for both of these effects in general terms by comparison with the characteristics of glass formation in simple fluids composed of small molecules or ions either when the experiments are performed very rapidly or when the experimental probe is at high frequencies.[31,32] For instance molecular dynamics computer simulation has been used to examine the transformation of the Lennard-Jones fluid into a glass by using cooling rates of the order 10^{12} s^{-1}.[33] Properties such as the expansivity show a gradual transformation from liquid to solidlike values over a temperature range of about half the temperature of the midpoint of the relaxation T_r. Also the value of T_r is high compared to that expected from a comparison with simple fluids on laboratory time scales.[31]

It has been shown[31,32] that these effects have nothing to do with the nature of the intermolecular potential since exactly the same qualitative effects have been seen experimentally when a property with a high characteristic frequency is used to probe the glass transition. For example, Brillouin scattering measurements have been used to probe sound velocity at frequencies of about 10 GHz in cooling experiments on the glass-forming liquid $2Ca(NO_3)_2{\cdot}3KNO_3$.[32] The high-frequency longitudinal compliance and the adiabatic compressibility derived from the measurements both show a smearing out of the transition to high temperature, while the more familiar static measurements show a sharp transition.

In both the fast-quenching and the high-frequency probe experiments the reasons for these phenomena are the same. First, as a sample is cooled structural relaxation rates begin to lag behind the rate of perturbation of the system at quite high temperatures, so the transformation starts well above the "normal" glass transition temperature. Second, these "fragile" fluids[34] show a marked temperature dependence of the activation energies (E_a) for structural relaxation processes. At low temperatures E_a becomes extremely large and relaxation times may change by 1 or 2 orders of magnitude over a few degrees—thus producing a very sharp transition. At high temperatures a much smaller value of E_a means that the same change occurs over a much wider temperature range—thus producing a broad transformation. Results suggest that it is the lower end of this range that seems to correspond with the transition temperature measured on the macroscopic time scale.

Glass formation in polymers is usually associated with the gradual freezing out of conformational fluctuations. Although it is not the intention in this paper to give a detailed discussion of the microscopic behavior of the model polymer, it is of relevance to note that the temperature dependence of the conformational distributions is in accord with the behavior discussed above. To perform this analysis we have determined the percentage of trans conformers for the unperturbed chains at various temperatures. We define a dihedral angle to be trans if it lies between ±60°, otherwise the angle is in one of the two gauche states. Averages obtained from all five samples in the temperature range 10–500 K are shown in Figure 8 together with the extra points obtained at 600 and 1000 K by heating just one sample to these temperatures. The solid line in the plot is an extrapolation to lower temperatures made on the basis of fitting the data at 500 and 1000 K to the form

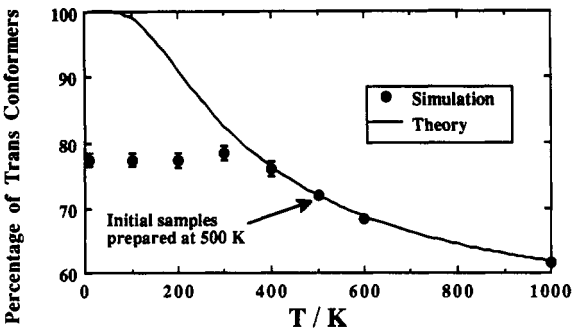

Figure 8. Percentage of trans conformers as a function of temperature for the unperturbed polymer samples prepared by either cooling or heating those generated at 500 K. The theoretical curve results from a fit of the data for the equilibrium constant at 500 and 1000 K to eq 16. The error bars shown are the standard deviations in the results for the five independent samples.

$$\langle X_T \rangle / \langle X_G \rangle = A \exp(\Delta\Phi/RT) \qquad (16)$$

where X denotes the fraction of trans (T) or gauche (G) states and A and $\Delta\Phi$ are the adjustable parameters. The actual values used for the curve shown were $A = 1.01$ and $\Delta\Phi/R = 463$ K. The nominal difference in energies between the gauche and trans wells for the dihedral angle potential is equivalent to 530 K, but this takes no account of the excluded-volume effects, which, for example, largely prevent sequences of the type G^+G^- from occurring. The low value of 463 K obtained simply implies an overall enhancement of the trans fraction.

Figure 8 clearly shows that on a time scale of about a nanosecond the torsional degrees of freedom fall out of equilibrium when the temperature is reduced below ~400 K. Indirectly the same phenomenon has been previously inferred[4] from the behavior of the end-to-end distance of short $N = 10$ and $N = 20$ alkane-like chains. The temperature at which this occurs correlates reasonably well with the temperature of the glass transformation, indicated in our case by the behavior of the modulus and disappearance of the yield stress. This result is in accord with the torsional degrees of freedom being the dominant modes of relaxation in these systems.

6. Conclusions

In this paper we have shown that the phenomenology of uniaxial deformation carried out at very high rates in computer experiments is very similar to typical results obtained in the laboratory on macroscopic samples and at much lower rates. The results show that phenomena such as elasticity, yield, and plastic flow are all accessible to dynamic atomistic modeling. The short time scale broadens the temperature range and reduces the magnitude of the changes observed as the material transforms from a viscoelastic fluid to an elastic solid.

The fact that a model as simple as a 1000-site chain filling space via the replicative properties of periodic

boundaries displays many of the characteristics of real systems is remarkable. The model can be easily extended to linear and branched polymers and to the study of, for instance, the chain length dependence of properties.

Acknowledgment. We thank E. I. du Pont de Nemours & Co., Inc., and I.C.I. plc for financial assistance and the S.E.R.C. for the provision of supercomputer time.

References and Notes

(1) Theodorou, D. N.; Suter, U. W. *Macromolecules* **1986**, *19*, 139; *Macromolecules* **1986**, *19*, 379.
(2) Mott, P. H.; Argon, A. S.; Suter, U. W. *Polym. Prepr.* **1989**, *30* (2), 34.
(3) Weber, T. A.; Helfand, E. *J. Chem. Phys.* **1979**, *71*, 4760.
(4) Rigby, D.; Roe, R. J. *J. Chem. Phys.* **1987**, *87*, 7285; *J. Chem. Phys.* **1988**, *89*, 5280; *Macromolecules* **1989**, *22*, 2259.
(5) Gao, J.; Weiner, J. H. *Macromolecules* **1989**, *22*, 979.
(6) Brown, D.; Clarke, J. H. R. *J. Chem. Phys.* **1986**, *84*, 2858.
(7) Brown, D.; Clarke, J. H. R. *Comp. Phys. Commun.*, in press.
(8) Berendsen, H. J. C.; Postma, J. P. M.; van Gunsteren, W. F.; DiNola, A.; Haak, J. R. *J. Chem. Phys.* **1984**, *81*, 3684.
(9) Hoover, W. G. *Phys. Rev. A* **1985**, *31*, 1695.
(10) Evans, D. J.; Holian, B. L. *J. Chem. Phys.* **1985**, *83*, 4069.
(11) Parrinello, M.; Rahman, A. *Phys. Rev. Lett.* **1980**, *45*, 1196.
(12) Nosé, S. *Mol. Phys.* **1984**, *52*, 255.
(13) Sylvester, M. F.; Yip, S.; Argon, A. S. *Polym. Prepr.* **1989**, *30* (2), 32.
(14) McKechnie, J. I.; Brown, D.; Clarke, J. H. R., manuscript in preparation.
(15) Byron Bird, R.; Curtiss, C. F.; Armstrong, R. C.; Hassager, O. Dynamics of Polymeric Liquids. *Fluid Mechanics*, 2nd ed.; Wiley: New York, 1987; Vol. 1 p 7.
(16) Sylvester, M., private communication.
(17) van der Ploeg, P.; Berendsen, H. J. C. *J. Chem. Phys.* **1982**, *76*, 3271.
(18) Steele, D. *J. Chem. Soc., Faraday Trans. II* **1985**, *81*, 1077.
(19) Richardson, M. J.; Flory, P. J.; Jackson, J. B. *Polymer* **1964**, *4*, 221.
(20) Allen, M. P.; Tildesley, D. J. *Computer Simulation of Liquids*; Clarendon Press: Oxford, 1987; p 147.
(21) Clarke, J. H. R.; Brown, D. *Mol. Sim.* **1989**, *3*, 27; N.B. See also: Clarke, J. H. R.; Brown, D. *Mol. Sim.* **1989**, *4*, 251; *Mol. Sim.* **1990**, *4*, 413.
(22) Reference 15, p 173.
(23) Ward, I. M. *Mechanical Properties of Solid Polymers*, 2nd ed.; Wiley: Chichester, 1985; p 331.
(24) Brown, N.; Ward, I. M. *J. Polym. Sci. A2* **1968**, *6*, 607.
(25) Reference 23, p 351. Rusch, K. C.; Beck, R. H., Jr. *J. Macromol. Sci.—Phys.* **1969**, *B3*, 365.
(26) Reference 23, p 337.
(27) Reference 23, p 376.
(28) Nielsen, L. E. *Trans. Soc. Rheol.* **1965**, *9.1*, 243. Newman, S.; Strella, S. *J. Appl. Polym. Sci.* **1965**, *9*, 2297. Litt, M. H.; Koch, P. J.; Tobolsky, A. V. *J. Macromol. Sci—Phys.* **1967**, *B1*, 587. Whitney, W.; Andrews, R. D. *J. Polym. Sci. C* **1967**, *16*, 2981.
(29) Reference 23; see, e.g., p 183.
(30) Hendra, P. J.; Jobic, H. P.; Holland-Moritz, K. J. *J. Polym. Sci., Polym. Lett. Ed.* **1975**, *12*, 365. Lam, R.; Geil, P. H. *J. Macromol. Sci.—Phys.* **1981**, *B20*, 37.
(31) Angell, C. A.; Clarke, J. H. R.; Woodcock, L. V. *Adv. Chem. Phys.* **1981**, *48*, 397.
(32) Angell, C. A.; Torrell, L. M. *J. Chem. Phys.* **1983**, *78*, 937.
(33) Clarke, J. H. R. *J. Chem. Soc., Faraday Trans.* **1979**, *2*, 1371.
(34) Angell, C. A. *J. Phys. Chem. Solids* **1988**, *49*, 863.